6-2009

Effects of Ultramicroelectrode Dimensions on the Electropolymerization of Polypyrrole

Benjamin J. Fletcher
University of Tennessee - Knoxville

Jared T. Fern
University of Tennessee - Knoxville

Kevin Rhodes
University of Tennessee - Knoxville

Timothy E. McKnight
Oak Ridge National Laboratory

Jason D. Fowlkes
University of Tennessee - Knoxville

See next page for additional authors

Recommended Citation

Benjamin L. Fletcher, Jared T. Fern, Kevin Rhodes, Timothy E. McKnight, Jason D. Fowlkes, Scott T. Retterer, David J. Keffer, Michael L. Simpson, and Mitchel J. Doktycz, J. Appl. Phys. (2010). Effects of ultramicroelectrode dimensions on the electropolymerization of polypyrrole 105, 124312 DOI:10.1063/1.3152633

Authors

Benjamin J. Fletcher, Jared T. Fern, Kevin Rhodes, Timothy E. McKnight, Jason D. Fowlkes, Scott T. Retterer, David J. Keffer, Michael L. Simpson, and Mitchel J. Doktycz

Effects of ultramicroelectrode dimensions on the electropolymerization of polypyrrole

Benjamin L. Fletcher,[1,2] Jared T. Fern,[3] Kevin Rhodes,[2] Timothy E. McKnight,[1,4] Jason D. Fowlkes,[1,2] Scott T. Retterer,[1,5,6] David J. Keffer,[3] Michael L. Simpson,[1,2,6] and Mitchel J. Doktycz[1,5,6,a)]

[1]*Molecular Scale Engineering and Nanoscale Technologies Research Group, Materials Science and Technology Division, Oak Ridge National Laboratory, Bethel Valley Road, Oak Ridge, Tennessee 37831, USA*
[2]*Materials Science and Engineering Department, University of Tennessee, 434 Dougherty Hall, Knoxville, Tennessee 37996, USA*
[3]*Chemical and Biomolecular Engineering Department, University of Tennessee, 1512 Middle Drive, Knoxville, Tennessee 37996, USA*
[4]*Monolithic Systems Group, Engineering Science and Technology Division, Oak Ridge National Laboratory, Oak Ridge, Tennessee 37831, USA*
[5]*Biological and Nanoscale Systems Group, Biosciences Division, Oak Ridge National Laboratory, Oak Ridge, Tennessee 37831, USA*
[6]*Center for Nanophase Materials Sciences, Oak Ridge National Laboratory, Oak Ridge, Tennessee 37831, USA*

(Received 24 October 2008; accepted 17 May 2009; published online 29 June 2009)

Anode geometry can significantly affect the electrochemical synthesis of conductive polymers. Here, the effects of anode dimensions on the electropolymerization of pyrrole are investigated. Band microelectrodes were prepared with widths ranging from 2 to 500 μm. The anode dimension has a significant effect on the resulting thickness of polymer film. The electropolymerization process deviates significantly from that predicted by simple mass transfer considerations when electrode dimensions are less than ~20 μm. Polymer film thickness is thinner than expected when electrode dimensions become less than ~10 μm. A simple mathematical model was derived to explain the observed effects of anode dimensions on the polymerization process. Simulation results confirm that diffusive loss of reaction intermediates accounts for the observed experimental trends. The described simulation facilitates understanding of the electropolymerization processes and approaches to the controlled deposition of polypyrrole, particularly at the submicron scale, for microelectromechanical systems and biomedical applications. © *2009 American Institute of Physics*. [DOI: 10.1063/1.3152633]

I. INTRODUCTION

Conductive polymers are attractive substitutes for the metallic conductors used in electronic devices. Since the report of Shirakawa *et al.*[1] on the electrical properties of oxidized polyacetylene, conductive polymers have been used as transistors,[2–5] microactuators,[6–8] and sensors.[9,10] The polymers are being synthesized on progressively smaller electrodes and, in some applications, the dimensions of the electrodes approach the submicron scale.[11,12] One of the more extensively examined conductive polymers is polypyrrole. It is readily prepared, chemically stable, and commercially available. Polypyrrole can be synthesized by either chemical or electrochemical techniques. Electrochemical methods, first described by Kanazawa *et al.*,[13] can be prepared at lower temperatures (25 °C) under aqueous conditions and result in higher quality polymer films when compared to chemical coating techniques.[14] These processing parameters also facilitate integration with biological structures.[12] Synthesis is initiated by electrochemically oxidizing the monomer. Applying a sufficiently positive potential on the anode generates radical cations that combine to form oligomers. A polymer film forms on the anode electrode surface as polymerization continues. The anode size, surface morphology, and activity influence the electropolymerization process.[15–17]

Electrodes are distinguished by their size and activity. Electrodes with a large surface area compared to the diffusion layer can alter the bulk concentration of electroactive species. In contrast, electrodes with relatively small surface areas compared to the solution volume do not substantially disturb the bulk solution. Ultramicroelectrodes (UMEs) are electrodes having one dimension, called the critical dimension, less than 25 μm.[18] The critical dimension of UMEs is smaller than the surrounding diffusion layer in unmixed systems. This relationship between the electrode and the surrounding diffusion layer has been found to dramatically impact the response of the system.[19–21] Analytically, large electrodes can be considered infinite or semi-infinite planes. Diffusion to the electrode surface can be modeled effectively by considering only transport normal to the substrate. In contrast, the relatively small size of UMEs requires consideration of diffusion in non-normal directions (i.e., not perpendicular, for band UMEs the range of directions is semicircular, approaching 2π). One consequence of this is that species generated at an UME can effectively "escape" from the electrode surface prior to participation in further

a)Electronic mail: doktyczmj@ornl.gov.

redox or chemical processes. In classic voltammetry of UMEs, this is observed by sigmoidal steady state oxidation (or reduction) voltammograms. For example, in a bulk solution of the reduced form of a reversible redox species, an anodic sweep will generate the oxidized species. Unless scan rates are fast enough to outpace this diffusive loss, these molecules can effectively escape from the electrode surface prior to the reverse cathodic sweep. The result of such escape is that there will be no significant cathodic wave at slow to moderate scan rates. For the electropolymerization of polypyrrole, this phenomenon can significantly influence the electropolymerization process. If the electrode is small enough, radical cations generated at the anode can quickly diffuse into the bulk solution where they do not participate in further reactions with the electrode surface. This diffusion-based phenomenon is likely to have a greater influence as electrode dimensions approach the submicron scale.

Here, the influence of band UME dimensions on the deposition of polypyrrole is explored. The critical dimension of the band electrode (width) is varied over a range of values (from 2 to 50 μm) and resulting polypyrrole films are evaluated. For comparison, a "point" electrode consisting of a carbon nanofiber (CNF) is also evaluated. The ability to finely tune the electrodeposition of polypyrrole films on the UMEs provides a means to tailor the size of and add advanced functionality to these structures in a highly controllable way. Polypyrrole composites have potential applications as nanoscale actuators,[22] microelectromechanical system devices,[6,7] as well as for various other electronic applications.[9,10,23,24] Insight into the effects of electrode size on the electrochemical behavior of UMEs will lead to better control of the electrodeposition process and will allow for nanoscale tailoring of electrode dimensions through polymer film deposition.

II. EXPERIMENTAL

A. Preparation of band ultramicroelectrodes

Arrays of band UMEs were produced using conventional microfabrication techniques. SiO_2 wafers (Silicon Quest International, Santa Clara, CA) were first spin coated with the photosensitive polymer, SPR 220 3.0 (Shipley, Marlborough, MA). UMEs were patterned using conventional photolithography techniques. The UMEs were spaced 500 μm apart to prevent cross talk between electrodes and were a range of widths (2–1000 μm). The UMEs were sufficiently long enough to be mathematically approximated as infinite in length. Layers of 10 nm titanium and 50 nm gold were deposited using electron beam evaporation and excess metal was lifted off in acetone.

UME arrays were connected to a common electrode and were simultaneously polymerized in 100 mM NaDBS (Sigma Aldrich, St. Louis, MO) and 100 mM pyrrole monomer (Sigma Aldrich, St. Louis, MO). A silver-silver chloride reference (3*M* KCl) and gold counter electrode were placed in solution and a constant 0.70 V potential was applied to the UME array for 20, 30, or 40 s. After rinsing, film thicknesses were measured by atomic force microscopy (AFM). The thickness of the underlying gold electrode (measured prior to polymerization) was subtracted from the total measured thickness.

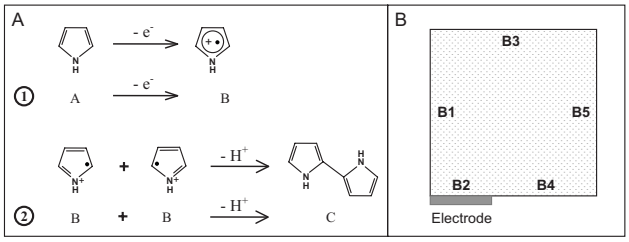

FIG. 1. Description of electrochemical reaction and system boundaries. (a) The chemical reactions and (b) system boundaries used in the mathematical model are shown. Reaction 1 represents the oxidation of reactants to radical intermediates and reaction 2 represents the combination of radical intermediates to form a polymer product. A symmetry boundary (B1), bulk solution (B3 and B5), the substrate (B4), and the electrode (B2) are represented by system boundaries.

B. Preparation of carbon nanofiber electrodes

To further reduce electrode dimensions, point UMEs were prepared from vertically aligned CNFs. Nickel catalyst metals were patterned and nanofibers were grown on metal-coated silicon wafers using previously described methods.[25–27] Briefly, silicon wafers (Silicon Quest International, Santa Clara, CA) were coated with a 50 nm layer of titanium for electrical connectivity. The metal-coated wafers were then spin coated with polymethyl methacrylate. Catalyst sites (dots 500 nm in diameter at a 5 μm pitch) were defined using UV-optical projection lithography (GCA AutoStep 200). Catalyst metal (50 nm Ni) was deposited by electron beam evaporation on the wafers and the excess metal was removed in an acetone lift-off. CNF growth was then performed using a plasma-enhanced chemical-vapor deposition process. Resulting nanofibers were, on average, 10 μm tall and 500 nm thick halfway between the base and the tip. The nanofibers were buried in a passivating polymer, SPR 220 7.0 (Shipley, Marlborough, MA), so that only the tips were exposed. As with the planar UMEs, the CNFs were immersed in 100 mM NaDBS and 100 mM pyrrole monomer. A silver-silver chloride reference (3*M* KCl) and gold counter electrode were placed in solution and a constant 0.70 V potential was applied for 20, 30, or 40 s. The passivating polymer was then dissolved in acetone and isopropyl alcohol, leaving a polypyrrole coating on the CNFs only at the exposed tips. Film thicknesses were measured using a scanning electron microscope. The thickness of the polypyrrole film was subtracted from the underlying thickness of the CNFs.

C. Mathematical model and simulations

A mathematical model was derived to generalize the polypyrrole polymerization reaction process. While the polypyrrole reaction system is well known within the literature,[14,28,29] a simplified reaction system, represented in Fig. 1(a), was used to evaluate the relationship between UME size and diffusive loss of polymerization products. Polymerization reactants (monomers and oligomers) are repre-

sented by composite reactant A. In reaction 1, these reactants are oxidized to form radical polymerization intermediates (radical cation forms of monomers and oligomers) represented by composite radical intermediate (B). Two radical intermediates combine in reaction 2 to form polymerization products (dimers and oligomers) represented by composite product (C). Concentrations of A, B, and C were modeled by coupled parabolic partial differential equations (PDEs)

$$\frac{\partial C_A}{\partial t} = D_A \nabla^2 C_A,$$

$$\frac{\partial C_B}{\partial t} = D_B \nabla^2 C_B - 2k_{bc} C_B^2,$$

$$\frac{\partial C_C}{\partial t} = D_C \nabla^2 C_C + k_{bc} C_B^2,$$

where C_A, C_B, and C_C represent the species concentrations in solution and D_A, D_B, and D_C represent diffusion coefficients for species A, B, and C, respectively. The reaction converting A to B only occurred at the boundary B2 and was represented by a constant flux. The reaction rate constant k_{bc} represents the rate at which B (radical intermediates) is converted to C (products). A diagram of the system boundaries is shown in Fig. 1(b). To simplify the model, a symmetry boundary (B1) was added. The polymerization reactions occur only at boundary B2 (representing the electrode). These reactions were modeled as a constant flux of A leaving the system and a constant flux of B entering the system. The assumption of constant flux of A to and B from the electrode is a simplification of a process which at the molecular level involves adsorption, reaction at the surface, and desorption. However, the experimentally observed dependence of polymer film thickness as a function of electrode size can be explained with some generality using this model, without specifying particular details of the adsorption isotherm or reaction kinetics at the electrode. For the work reported here, the flux of A to the surface and the flux of B from the surface are equal in magnitude, representative of a steady-state process. Boundaries B3 and B5 represent bulk concentrations of species. At these boundaries, C_B and C_C are equal to 0 and C_A is equal to 1, where all concentrations are represented by C/C_A^O. Boundary B4 is the substrate and is assumed to be impermeable (flux is 0).

The software package FEMLAB (v3.0) was used to numerically solve the system of coupled, nonlinear PDEs by finite element analysis. The system was solved for a total of 5 s with a step size of 0.05 s. To determine if the electrode width affected the concentration of reaction products (C), a series of simulations were performed with different electrode widths. The simulated electrode widths were $\frac{1}{2}$ of the actual electrode widths since the boundary B4 is a symmetry boundary. Simulated electrode widths normalized by the total box width (l_{ele}/L_{box}) were 0.05, 0.025, 0.02, 0.015, 0.01, 0.005, and 0.002. For each electrode width, the mesh was reevaluated and refined around the electrode (B2) with a maximum element size of 0.0005, leaving at least four elements along the electrode boundary for all electrode sizes.

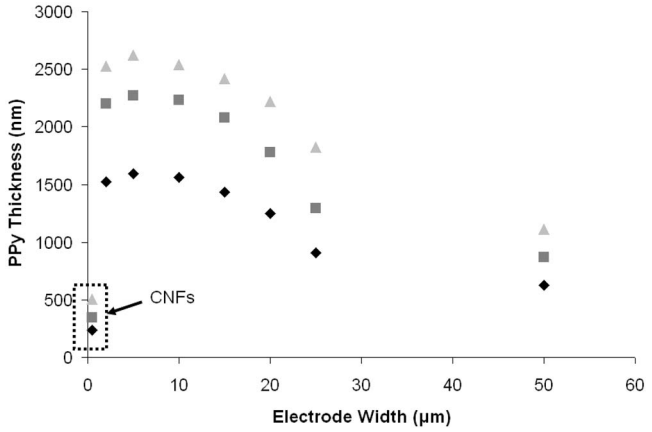

FIG. 2. Polypyrrole film thickness as a function of electrode width. Polypyrrole film thickness was measured using UMEs of varying widths (2–50 μm). The polymerization reaction time for data points represented by (♦) was 20 s, for data points represented by (■) was 30 s, and for data points represented by (▲) was 40 s. Film thicknesses measured from CNF electrodes are also included (data points in dashed box).

The default mesh was utilized everywhere else. The average concentration of C_C/C_A^O along the electrode relative to B1 was used when reporting the concentration of C on the electrode at the end of each analysis.

The diffusivities of components A, B, and C were assumed to be constant and are given by $D_A=1$, $D_B=\frac{1}{2}$, and $D_C=1/3$ (relative to D_A). The unitless flux $[N/(C_A^O D_A)]$ of A leaving the system and B entering the system is equal to -2 and 2, respectively. The rate constant for the reaction represented by k/k_{max} was varied over four orders of magnitude from 0.001 to 1.

III. RESULTS AND DISCUSSION

Polypyrrole was electrochemically deposited on the surfaces of an array of band UMEs with different widths. The thicknesses of the deposited polypyrrole films were then measured by AFM. Shown in Fig. 2 are graphs of the film thickness measurements versus UME widths for three different polymerization times. Starting with the largest electrode (50 μm wide), PPy film thicknesses on the surfaces of the UMEs increase as the electrode widths decrease. In Fig. 2, polymer films are increasingly thicker for electrode widths between 20 and 50 μm. This matches the behavior predicted by the mass transfer equation for band UMEs,

$$m_o = (2\pi D_o)/[w \ln(64 D_o t/w^2)], \quad (1)$$

where D_o is the diffusion coefficient, t is time, and w is the width of the band UME.[18] The mass transfer coefficient m_o is a proportionality constant ($m_o=D_o/\delta_o$, where δ_o is the thickness of the Nernst diffusion layer) and has units of cm/s (the same as a rate constant of a first-order heterogeneous reaction). However, deviations from predicted behavior are observed for electrode widths less than ~20 μm. At electrode widths less than ~10 μm, measured film thicknesses actually begin to decrease with further decreases in width. Further reductions in electrode dimensions result in less buildup of polymer on the electrode surfaces.

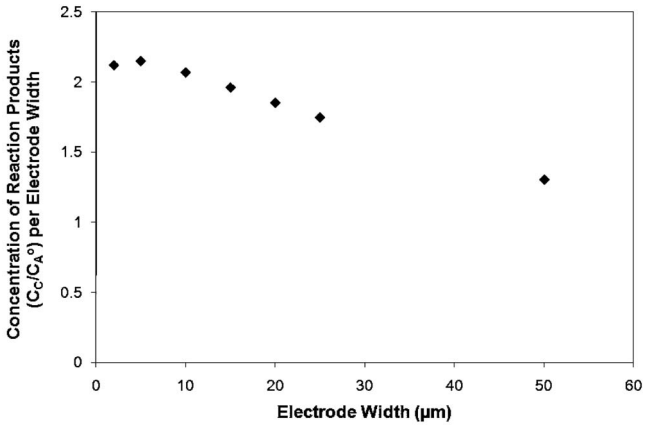

FIG. 3. Reaction product concentration at surface as predicted from simulation. Simulation results are based on the described reaction model. The concentration of reaction products (C) at the electrode surface (B2) is plotted as a function of electrode width. Concentrations are expressed as (C_C/C_A^o)/electrode width.

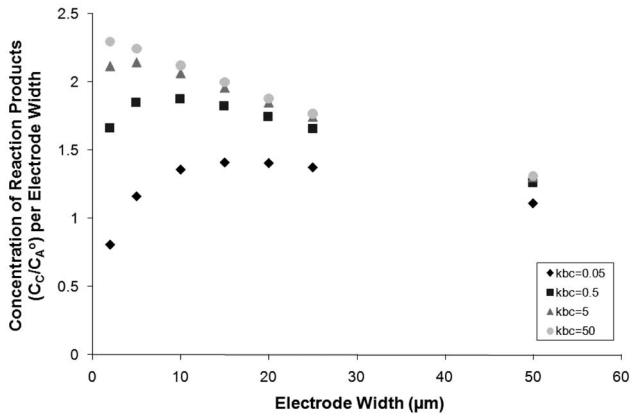

FIG. 4. Simulation results summarizing the effects of changing composite production rate. The effects of varying the rate, k_{bc}, that B reacts to produce C within the reaction model system are shown. Concentrations are expressed as (C_C/C_A^o)/electrode width.

Data from CNF-based point electrodes are also included with the data from the band UMEs in Fig. 2 to illustrate that the trend extends to electrodes with nanoscale dimensions. Although CNF electrodes were constructed from a different material and possess a different geometry, their inclusion in the data indicates that polymer film thicknesses continue to decrease as electrode dimensions are reduced to less than 10 μm wide. Clearly, the electropolymerization process is affected by the size of the electrode. The polymer deposition process can no longer be predicted by Eq. (1) for band electrodes less than 20 μm wide or for a nanoscale point electrode. A likely explanation for this unusual behavior is the diffusion of radical cations and oligomers into the bulk solution before reacting with the electrode surface.

A mathematical model was derived to generalize the polymerization reaction system to test this hypothesis. Simulations based on the model provided concentrations of A, B, and C as a function of two-dimensional spatial coordinates. The electrode was modeled as an ideal UME with an exposed electrode area planar to the substrate. While experimental data were collected from nonideal UMEs, elevated 60 nm above the substrate, previous studies have demonstrated that this nonideal, elevated electrode profile has a negligible effect on electrochemical reactions relative to the other electrode dimensions (width and length).[30] Thus, in our simulations, the electrodes could be effectively approximated by ideal planar UMEs. It was assumed that the current density at the electrode surface and the affinity of *C* to adhere to the electrode are independent of changes in electrode dimensions. If true, the thickness of the PPy film that forms on the electrode could be determined by the concentration of *C* at B2. The concentration of *C* as a function of electrode width was integrated along B1 up to 0.05 above the electrode (normalized by the total box width). Any species C beyond this point was assumed to be lost to the bulk solution. Results are plotted versus electrode width and can be seen in Fig. 3. The concentration of *C* around the electrode increases with decreasing electrode width until ~10 μm, where the concentration begins to deviate from behavior predicted by the simple mass transfer equation. At ~5 μm, the concentration of *C* begins to decrease with further decreases in electrode width. The general behavior matches the trends observed in the experimental data in Fig. 1, suggesting that the simplified model and the assumptions made are valid.

Small discrepancies in the inflection points of the simulation data and the experimentally observed results are due to the choice of model parameters (D, k_{bc}, etc.). A parametric sensitivity analysis was performed for the diffusivities, the fluxes to the electrode surface, and the composite reaction rate constant. Essentially there are three processes at work in this system: the conversion of A to B [reaction 1 in Fig. 1(a)], the conversion of B to C [reaction 2 in Fig. 1(a)], and the diffusion of B from the electrode. The key competition in terms of understanding the relationship between film thickness and electrode size is between the second and third processes. In order to obtain thick films, the conversion of B to C must dominate over the diffusion of B from the electrode. Thus we expect that fast conversion (large k_{bc}) and slow diffusion (small D_B) will favor thick films for small electrodes. The rate of production of B via reaction will certainly affect the film thickness but should not change as a function of electrode size.

In the model, the most straightforward case is to assume that the surface reaction for conversion of A to B is at steady state, where the flux of A to the surface and the flux of B from the surface are equal in magnitude. In this case, changes to the rate that monomer A is converted to radical cation B change the amount of B in the system. However, the ultimate fate of this intermediate is dependent on whether it diffuses away from the electrode before it can react to form C. Therefore, the more interesting parameters to vary are those that directly affect the rates of diffusion of B and conversion of B.

The effects of changing the diffusion coefficient of the radical cations D_B were investigated. As the diffusion coefficient was increased, large deviations from the predictions of Eq. (1) occur. This can be attributed to the diffusion of B from the electrode. Conversely, we can vary the rate of consumption of B. In Fig. 4, the effects of varying the rate that

B reacts to produce C (k_{bc}) over four orders of magnitude are illustrated. As the reaction rate is reduced, the amount of C generated at B2 is reduced and deviations from predicted behavior (Eq. (1)) are observed for electrode widths less than 15 μm. This again can be understood in terms of the competition between diffusion and reaction. For slow composite reaction kinetics, the intermediates can diffuse away before reacting. As the size of the electrode decreases, the directions in which the intermediates can diffuse away increase, resulting in a decrease in film thickness. The same principles apply for the competition between diffusion and reaction for both small and large species.

The model's responses to changes in reaction parameters support the assumption that polypyrrole film thickness is dependent on the concentration of intermediates surrounding the electrode. In turn, the local concentration of C is dependent on the competition between diffusion and the electropolymerization reaction rate. As the electrode size becomes smaller, the availability of diffusive paths away from the electrode becomes more significant and leads to deviation from the behavior predicted by Eq. (1). In the case of polypyrrole polymerization, enhanced diffusion of the reaction intermediates B and C away from the UME surfaces results in lower polymer film thicknesses.

IV. CONCLUSIONS

It is well established that mass transfer around UMEs dramatically increases with decreasing electrode size [Eq. (1)]. This increased mass transfer can have significant impact upon the electropolymerization process, whereby electrochemically generated species can be diffusively lost to the surrounding bulk solution prior to participating in the electrodeposition process at the electrode surface. We anticipated this diffusive loss of electrochemical reaction products to the bulk solution could be a significant factor in the electrodeposition of polypyrrole upon UMEs. To confirm this, band UMEs of a range of different widths were used to electropolymerize pyrrole. Resulting polymer film thicknesses were evaluated by AFM. Deposition of polypyrrole on the UMEs increased as electrode widths were decreased from 50 down to ~10 μm. At electrode widths less than ~10 μm, measured film thicknesses began to decrease with further decreases in width. This trend continued for nanoscale electrodes where the tips of CNFs were used as point electrodes for the electropolymerization of polypyrrole. The thickness of the deposited polymer on the nanofibers indicates that the trend extends to the nanoscale.

A simple mathematical model was used to help visualize the interplay between increased mass transfer and the composite chemical reaction steps that must occur in the formation of a polymer film on the electrode surface. Simulation results replicated the trends observed in the experimental data based on variation in species' diffusivity and generalized composite reaction rates of the subsequent polymerization process. The combined results from experiments and simulations indicate that for the diffusivities and reaction rates of a common PPy electrodeposition process (100 mM pyrrole in 100 mM NaDBS), reaction intermediate loss from participation in polymerization at the electrode surface is significant at electrode sizes below ~10 μm. It should be noted that our model did not incorporate consideration of charge effects between the electrode and the cationic oxidized pyrrole radical. It is anticipated that such charge effects also have a role in the accumulation of PPy on the electrode due to known electrostatic interactions of the oxidized radical.[31] Additional work, whereby charge effects are reduced by using higher concentrations of supporting electrolytes, could be used to evaluate these effects. However, diffusive loss of reaction products to the bulk solution appears to be the dominant process at electrode dimensions of <10 μm. These findings are in agreement with previously described UME behavior,[20,21] and it is important that these phenomena be accounted for in applications requiring the electrodeposition of polypyrrole on UMEs.

ACKNOWLEDGMENTS

This research was supported by NIH (Grant No. EB000657). A portion of this research was conducted at the Center for Nanophase Materials Sciences, which is sponsored at Oak Ridge National Laboratory by the Division of Scientific User Facilities, U.S. Department of Energy. M.L.S. acknowledges the support from the Materials Sciences and Engineering Division Program of the DOE Office of Science. This work was performed at the Oak Ridge National Laboratory, managed by UT-Battelle, LLC, for the U.S. DOE under Contract No. DE-AC05-00OR22725.

[1] H. Shirakawa, E. J. Louis, A. G. MacDiarmid, C. K. Chiang, and A. J. Heeger, J. Chem. Soc., Chem. Commun. **1977**, 578.
[2] C. D. Dimitrakopoulos and P. R. L. Malenfant, Adv. Mater. **14**, 99 (2002).
[3] D. J. Gundlach, Y. Y. Lin, T. N. Jackson, S. F. Nelson, and D. G. Schlom, IEEE Electron Device Lett. **18**, 87 (1997).
[4] O. Mermer, G. Veeraraghavan, T. L. Francis, Y. Sheng, D. T. Nguyen, M. Wohlgenannt, A. Kohler, M. K. Al-Suti, and M. S. Khan, Phys. Rev. B **72**, 205202 (2005).
[5] M. Shtein, J. Mapel, J. B. Benziger, and S. R. Forrest, Appl. Phys. Lett. **81**, 268 (2002).
[6] E. Smela, J. Micromech. Microeng. **9**, 1 (1999).
[7] E. Smela, Adv. Mater. **15**, 481 (2003).
[8] E. Smela and N. Gadegaard, J. Phys. Chem. B **105**, 9395 (2001).
[9] J. H. Burroughes, D. D. C. Bradley, A. R. Brown, R. N. Marks, K. Mackay, R. H. Friend, P. L. Burns, and A. B. Holmes, Nature (London) **347**, 539 (1990).
[10] O. A. Sadik, Electroanalysis **11**, 839 (1999).
[11] J. H. Chen, Z. P. Huang, D. Z. Wang, S. X. Yang, J. G. Wen, and Z. Ren, Appl. Phys. A: Mater. Sci. Process. **73**, 129 (2001).
[12] B. L. Fletcher, T. E. McKnight, J. D. Fowlkes, D. P. Allison, M. L. Simpson, and M. J. Doktycz, Synth. Met. **157**, 282 (2007).
[13] K. K. Kanazawa, A. F. Diaz, R. H. Geiss, W. D. Gill, J. F. Kwak, J. A. Logan, J. F. Rabolt, and G. B. Street, J. Chem. Soc., Chem. Commun. **1979**, 854.
[14] A. F. Diaz and J. Barcon, *Handbook of Conducting Polymers* (Marcel Dekker, New York, 1986), Vol. 1.
[15] S. Biallozor and A. Kupniewska, Synth. Met. **155**, 443 (2005).
[16] M. Schirmeisen and F. Beck, J. Appl. Electrochem. **19**, 401 (1989).
[17] M. F. Suarez and R. G. Compton, J. Electroanal. Chem. **462**, 211 (1999).
[18] A. J. Bard and L. R. Faulker, *Electrochemical Methods: Fundamentals and Applications* (Wiley, New York, 2001).
[19] C. Amatore and I. Svir, J. Electroanal. Chem. **557**, 75 (2003).
[20] M. V. Mirkin and A. J. Bard, J. Electroanal. Chem. **323**, 1 (1992).
[21] C. P. Smith and H. S. White, Anal. Chem. **65**, 3343 (1993).
[22] B. L. Fletcher, S. T. Retterer, T. E. McKnight, A. V. Melechko, J. D. Fowlkes, M. L. Simpson, and M. J. Doktycz, ACS Nano **2**, 247 (2008).
[23] A. F. Diaz and J. I. Castillo, J. Chem. Soc., Chem. Commun. **1980**, 397.

[24]R. H. Friend, R. W. Gymer, A. B. Holmes, J. H. Burroughes, R. N. Marks, C. Taliani, D. D. C. Bradley, D. A. Dos Santos, J. L. Bredas, M. Logdlund, and W. R. Salaneck, Nature (London) **397**, 121 (1999).
[25]A. V. Melechko, V. I. Merkulov, T. E. McKnight, M. A. Guillorn, K. L. Klein, D. H. Lowndes, and M. L. Simpson, J. Appl. Phys. **97**, 041301 (2005).
[26]V. I. Merkulov, D. H. Lowndes, Y. Y. Wei, G. Eres, and E. Voelkl, Appl. Phys. Lett. **76**, 3555 (2000).
[27]Z. Ren, Z. P. Huang, D. Z. Wang, J. G. Wen, J. W. Xu, J. H. Wang, L. E. Calvet, J. Chen, J. F. Klemic, and M. A. Reed, Appl. Phys. Lett. **75**, 1086 (1999).
[28]C. P. Andrieux, P. Audebert, P. Hapiot, and J. M. Saveant, J. Phys. Chem. **95**, 10158 (1991).
[29]S. Sadki, P. Schottland, N. Brodie, and G. Sabouraud, Chem. Soc. Rev. **29**, 283 (2000).
[30]J. A. Alden and R. G. Compton, Electroanalysis **8**, 30 (1996).
[31]A.-H. Bae, T. Hatano, M. Numata, M. Takeuchi, and S. Shinkai, Macromolecules **38**, 1609 (2005).